ChemPubSoc Europe
DOI: 10.1002/cptc.201900118
CHEMPHOTOCHEM Concepts

Aggregation-Induced Delayed Fluorescence

Hao Liu,[a] Jingjing Guo,[a] Zujin Zhao,*[a] and Ben Zhong Tang[a, b]

The huge market demand for organic light-emitting diodes (OLEDs) has attracted a significant number of researchers to explore robust and cheap luminescent materials for application in high-performance and low-cost OLEDs. This concept article presents a new class of organic luminescent materials which demonstrate aggregation-induced delayed fluorescence (AIDF). This material type can perform particularly well when applied in nondoped OLEDs, with devices exhibiting excellent electroluminescence (EL) efficiencies and very small efficiency roll-off. Recent works on typical AIDF materials, investigating molecular design strategies, photophysical properties and EL performance in nondoped OLEDs, are discussed. These newly emerged organic luminescent materials are promising candidates for highly efficient nondoped OLEDs and have potential practical applications.

1. Introduction

Thermally activated delayed fluorescence (TADF) materials with pure and organic ingredients have shown great potentials in organic light-emitting diodes (OLEDs) because of their high exciton utilization and low cost.[1] These TADF materials possess small energy splitting ($\triangle E_{ST}$) between the lowest singlet excited state (S_1) and the lowest triplet excited state (T_1), which can overcome the spin statistical limit of 25% on the singlet production yield through reverse intersystem crossing (RISC).[2] However, most TADF emitters suffer from severe concentration-caused emission quenching and exciton annihilation. In consequence, they generally have to be dispersed in proper host matrices to alleviate these problems. The doped OLEDs based on TADF emitters indeed have achieved enhanced electroluminescence (EL) efficiencies with exciton utilization approaching unity at low voltages, but these devices always encounter a troublesome problem of serious efficiency roll-off as the luminance increases, which remains as an obstacle to their widespread commercial application in OLED industry.[3] Recently, several robust TADF emitters that could inhibit concentration quenching had been developed and used to fabricate nondoped OLEDs. The efficiency roll-off of these nondoped OLED could been reduced to a large extent,[2a,4] implying that the nondoped OLEDs based on TADF emitters may have potential to increase efficiency stability of the devices.

Aggregation-induced emission (AIE) refers to an interesting luminescent phenomenon that nonfluorescent or weakly fluorescent molecules in solutions are induced to emit strong photoluminescence (PL) by aggregate formation.[5] Luminogens with AIE property (AIEgens) are free of aggregation-caused quenching and can fluoresce efficiently in neat films.[6] AIEgens generally possess highly twisted molecular structures and experience weak intermolecular interactions in the aggregated state, which is conducive to suppressing exciton annihilation and efficiency roll-off. To date, many AIEgens have been demonstrated to be suitable to fabricate stable nondoped OLEDs. However, the majority of AIEgens are intrinsically fluorescent molecules, and thus can only harness singlet excitons for light emission, resulting in theoretically maximum external quantum efficiency (EQE_{max}) of only 5.0~7.5% for the OLEDs. Hence, endowing AIEgens with new exciton utilization mechanism, such as TADF, triplet-triplet annihilation (TTA) and hybridized local and charge-transfer (HLCT), can be a feasible strategy to break the bottleneck constraint of low exciton utilization of AIEgens.

The highly twisted molecular structures of AIEgens and TADF emitters are essentially compatible. And actually, some TADF emitters have AIE property in nature, that is the PL quantum yields (PLQYs) of these molecules in solid state can be much higher than those in solutions.[7] It is also reported that the intermolecular charge transfer that is facilitated in solid state can also improve the RISC transitions and therefore enhance the delayed fluorescence.[8] In 2015, Chi et al. designed a series of AIEgens consisting of electron-withdrawing diphenylsulfone, and electron-donating carbazole and phenothiazine (PTZ). These interesting AIEgens exhibited apparent delayed fluorescence and excellent mechanoluminescence, and could provide white PL emission by morphological control of the aggregate.[9] However, the application of these materials in nondoped OLEDs were not reported. In 2016, our group also initially developed several molecules that combined the AIE and delayed fluorescence by introducing electron-donating phenoxazine (PXZ) and PTZ onto electron-withdrawing dibenzothiophene-S,S-dioxide.[10] In 2016, Yasuda et al. reported three new *o*-carborane-based molecules that held both AIE and TADF properties, and the two emission behaviors were called as

[a] H. Liu, J. Guo, Prof. Z. Zhao, Prof. B. Z. Tang
State Key Laboratory of Luminescent Materials and Devices
Center for Aggregation-Induced Emission
South China University of Technology
Guangzhou 510640 (China)
E-mail: mszjzhao@scut.edu.cn
[b] Prof. B. Z. Tang
Department of Chemistry, Hong Kong Branch of Chinese National Engineering Research Center for Tissue Restoration and Reconstruction
The Hong Kong University of Science & Technology
Clear Water Bay, Kowloon, Hong Kong (China)

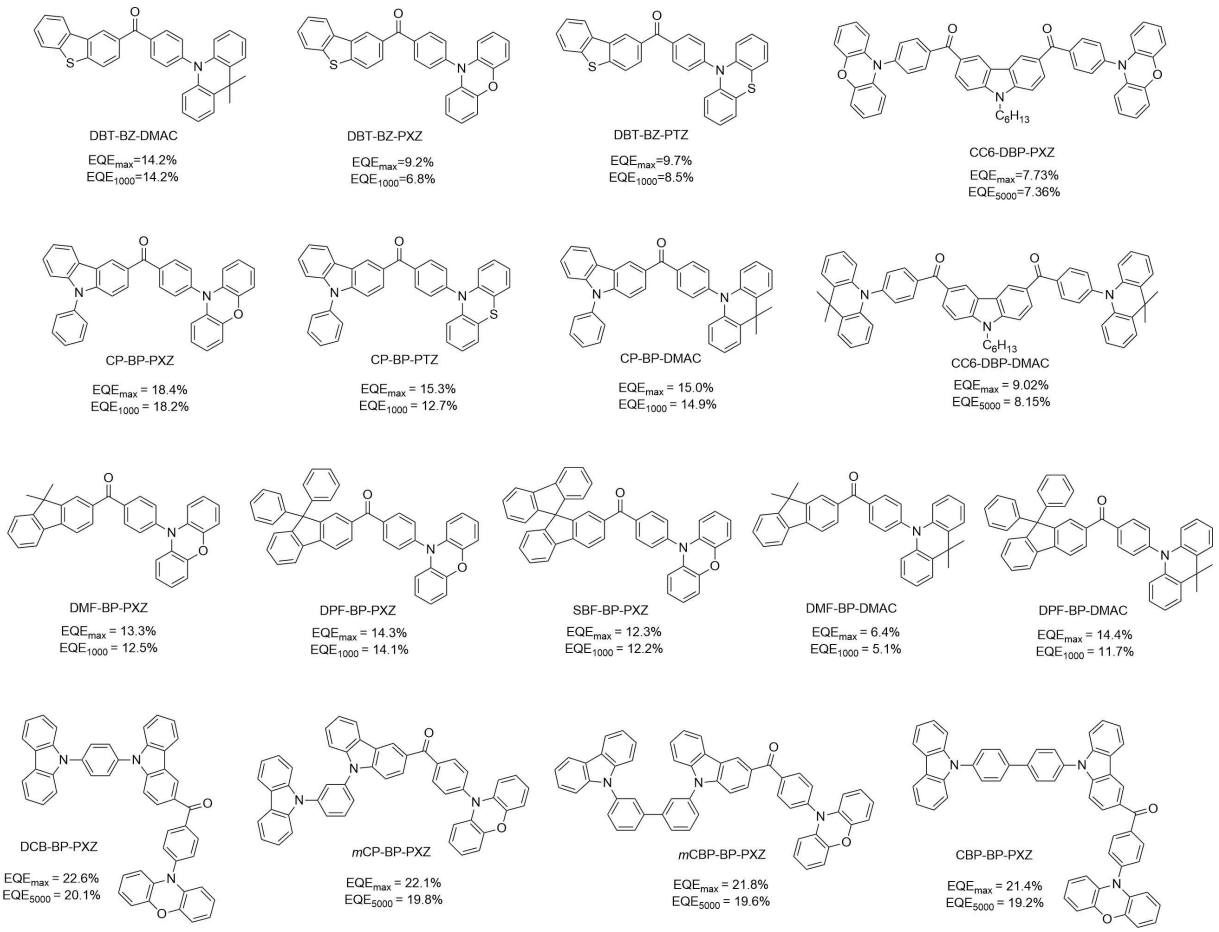

Figure 1. Molecular structures of representative AIDF materials containing a benzophenone core and key performance parameters: maximum EQE (EQE_{max}), and EQE at 1000 cd m^{-2} (EQE_{1000}) or at 5000 cd m^{-2} (EQE_{5000}).

aggregation-induced delayed fluorescence (AIDF).[11] They successfully demonstrated the good potential of these molecules in the fabrication of nondoped OLEDs, although there were still much space for the further improvement of device performances in view of relatively low EQE_{max} of 11% and large efficiency roll-off.

In 2017, we explored a novel class of AIDF materials that had an asymmetrical electronic donor-acceptor-donor′ (D-A-D′) structures comprised of an electron-withdrawing ketone and various electron-donating groups. We further approved the feasibility of these AIDF materials for the fabrication of nondoped OLEDs to increase EL efficiencies and reduce efficiency roll-off. More importantly, we found that the definition of AIDF was not just the statement combination of AIE and TADF. The AIDF phenomenon actually had its own implication, as it stood for a unique photophysical process that the materials exhibited weak fluorescence with negligible delayed component in solutions, but emitted strongly with distinct delayed fluorescence upon aggregate formation or in neat films. We depicted the underlying mechanism by transient absorption and fluorescence spectroscopies, and theoretical calculations. By further molecular engineering, the performances of our AIDF materials had greatly boosted, presenting many merits of high solid-state PLQY, nearly 100% exciton harvesting and low cost. The nondoped OLEDs based on our AIDF materials could provide impressive EL efficiencies comparable to those of the doped OLEDs based on common TADF emitters. In particular, the efficiency roll-off of nondoped OLEDs of AIDF materials was extremely small, which shed light on solving the severe efficiency roll-off problem of TADF materials. Therefore, AIDF materials may have great potentials to be the most promising emitters for the fabrication of high-performance nondoped OLEDs. In this concept article, we focus on the representative achievements in the rapidly developing area of AIDF materials, emphasizing the molecular design, mechanism understanding and applications in nondoped OLEDs. An outlook for the AIDF systems is also presented, hoping to make a contribution to nondoped OLEDs.

2. Representative AIDF Materials and Mechanism

The electron-withdrawing benzophenone (BP) is an efficient building block for the construction of TADF emitters.[12] The typical AIDF materials were just created based on this simple-structured BP core (Figure 1). Initially, an asymmetrical D-A-D′

molecule, DBT-BZ-DMAC, was designed by attaching electron-donating dibenzothiophene (DBT) and 9,9-dimethyl-9,10-dihydroacridine (DMAC) to the BP core.[13] DBT-BZ-DMAC was a weak emitter in tetrahydrofuran (THF) solution with a low PLQY of 8.3%. It exhibited strong green PL at 505 nm with a high PLQY of 80.2% in neat film, which was higher than those in doped films at different doping concentrations (60.6–79.0%). More interestingly, the $\triangle E_{ST}$ in doped film was decreased as the doping concentration increased, and reached a minimum (0.08 eV) in neat film, indicating that the neat film was favorable for the occurrence of delayed fluorescence. Indeed, the rate of RISC (k_{RISC}) was increased as the doping concentration became higher. In neat film it was nearly $27.5\times10^4\ s^{-1}$, which was much higher than that in 6 wt% doped film ($3.23\times10^4\ s^{-1}$). And the delayed lifetime in neat film was 2.9 μs, being much shorter than that in 6 wt% doped film (20.4 μs). We thought that the short lifetime of delayed fluorescence indicated that the triplet excitons could be quickly up-converted to singlet excitons for light emission via RISC process in OLEDs, which could be an efficient method to suppress the bimolecular quenching process, such as TTA, of high-concentration excitons, and thus reduce efficiency loss at high voltages (Figure 3). The nondoped OLED with a very simple configuration of indium tin oxide (ITO)/TAPC (25 nm)/DBT-BZ-DMAC (35 nm)/TmPyPB (55 nm)/LiF (1 nm)/Al was fabricated, in which the DBT-BZ-DMAC neat film functioned as the light-emitting layer, 1,1′-bis(di-4-tolylaminophenyl) cyclohexane (TAPC) served as the hole-transporting layer and 1,3,5-tri(*m*-pyrid-3-yl-phenyl)benzene (TmPyPB) worked as the electron-transporting layer. The turn-on voltage of this nondoped OLED was 2.7 V, indicative of efficient carrier injection and transport. The nondoped OLED showed EQE_{max}, maximum current efficiency (CE_{max}) and maximum power efficiency (PE_{max}) of 14.2%, 43.3 cd A^{-1} and 35.7 lm W^{-1} with extremely small roll-off of 0.46% at 1000 cd m^{-2}.

To confirm the advantages of AIDF materials in the fabrication of nondoped OLED, doped OLEDs with varied doping concentration ranging from 6 wt% to 90 wt% of DBT-BZ-DMAC doped in 4,4′-di(9H-carbazol-9-yl)-1,1′-biphenyl (CBP) matrix were fabricated. It was found that, as the increase of doping concentration, the EQE_{max} of doped OLED was increased in some degree but the efficiency roll-off was greatly reduced and reached minimum in neat film. For example, the doped OLED with a low doping concentration of 6 wt% showed a higher EQE_{max} of 17.9% and larger efficiency roll-off of 39.8% at 1000 cd m^{-2}, while the device with a high doping concentration of 90 wt% gave a lower EQE_{max} of 13.4% and a smaller efficiency roll-off of 2.04% at 1000 cd m^{-2}, which meant that the later device could function more efficiently than the former one at high voltages.

Actually, this was not the only case we found in our preliminary studies. By replacing DMAC donor with the PXZ or PTZ units, the new molecules DBT-BZ-PXZ and DBT-BZ-PTZ showed similar AIDF property, and their nondoped OLEDs also gave very small efficiency roll-off.[14] Moreover, a library of D-A-D′ molecules consisting of 9,9-dimethylfluorene (DMF), 9,9-diphenylfluorene (DPF) and 9,9′-spirobifluorene (SBF), PXZ and DMAC as electron donor, and BP as acceptor had been demonstrated to hold AIDF property. The nondoped OLEDs adopting these AIDF materials as light-emitting layers enjoyed very small efficiency roll-off as well. For instance, the PLQY of DPF-BP-DMAC in neat film was 62.3%, much higher than that in solution.[15] It also showed a longer lifetime of delayed component in neat film than in solution, revealing the prominent AIDF characteristic. The nondoped OLEDs based on DPF-BP-DMAC afforded good EQE_{max}, CE_{max} and PE_{max} of 14.4%, 42.3 cd A^{-1} and 30.2 lm W^{-1}, respectively. And the efficiency roll-off was as small as 4.5%. These results disclosed that the AIDF property had successfully suppressed the high-concentration exciton annihilation and thus reduced efficiency roll-off at high luminance to a large extent. Although the EL efficiencies of these AIDF materials were inferior to those of the art-of-state TADF emitters, the greatly reduced efficiency roll-off of these nondoped OLEDs was a distinct merit that TADF materials desired, which was of great importance for the practical application.

In view of the bright future of AIDF materials, we wondered the fundamental mechanism underlying AIDF phenomenon, which is important to rational design of more efficient AIDF materials.[16] Taking DMF-BP-PXZ as an example, it showed faint emission in THF solution with a low PLQY of 2.6% and a short lifetime of 2.3 ns, and no discernable delayed fluorescence was observed, but exhibited bright luminescence and notable delayed fluorescence along with the aggregate formation (Figure 2). And in solid film, it luminesced more strongly, giving a high PLQY of 45.4% and a long lifetime of delayed fluorescence of 1.4 μs. It was found that its internal conversion rate (k_{IC}) in neat film ($1.3\times10^7\ s^{-1}$) was much smaller than that in solution ($4.17\times10^8\ s^{-1}$), which was mainly ascribed to the restriction of intramolecular motion in neat films. The nanosecond transient absorption spectrum in solution showed no absorption peak of triplet state, in accordance with the lack of delayed fluorescence in solutions. But in neat film, DMF-BP-PXZ showed apparent absorption peak of triplet state, with a long lifetime of 1.41 μs, clearly demonstrating that DMF-BP-PXZ was more ready to achieve triplet via intersystem crossing (ISC) process in the solid state. Density functional theory, time-dependent density functional theory simulations and the combined quantum mechanics and molecular mechanics (QM/MM) methods were employed to deeply depict the underlying mechanism of the emission property in solutions and solid states. The calculated results disclosed that the k_{IC} of DMF-BP-PXZ in solid was $8.81\times10^6\ s^{-1}$, which was significantly reduced relative to that in solution ($3.06\times10^{10}\ s^{-1}$). This finding was consistent with the experimental results. In addition, in solid, the intersystem crossing rate (k_{ISC}) and k_{RISC} were $6.6\times10^6\ s^{-1}$ and $7.2\times10^4\ s^{-1}$, respectively. The k_{ISC} could compete against k_{IC}, leading to the occurrences of ISC, RISC and thus delayed fluorescence. Moreover, the value of spin orbit coupling (SOC) was increased and energy difference between triplet and singlet states was decreased in solid in comparison with those in solution, both of which could facilitate the ISC process, and were conducive to delayed fluorescence. These results revealed the efficient suppression of internal conversion (IC) channel

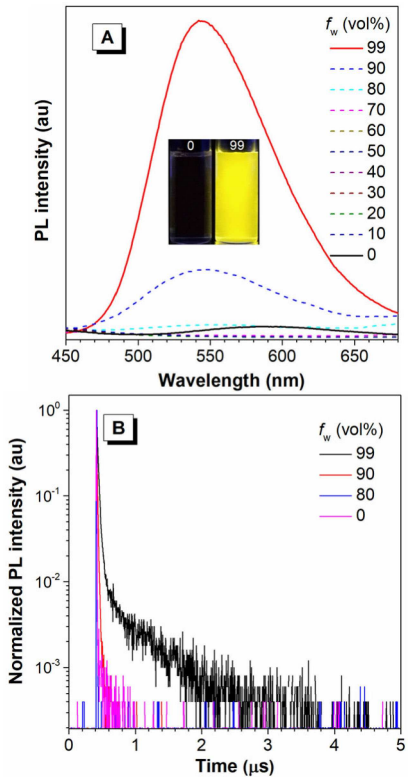

Figure 2. (A) Photoluminescence (PL) spectra and (B) transient PL decay spectra of DMF-BP-PXZ in THF/water mixtures with different water fractions (f_w), measured under nitrogen. Inset in (A): photos of DMF-BP-PXZ in THF/water mixtures ($f_w = 0$ and 99%), taken under illumination with a 365 nm UV lamp. Adapted with permission from Ref. [16], copyright 2018 Wiley-VCH.

and enhanced k_{ISC} in the aggregated state, which were favored to generate delayed fluorescence. So, a picture of AIDF mechanism became clearly that in solution state, the dominative IC process killed the singlet excited state in a nonradiative manner before the ISC process occurred, leading to neither prompt fluorescence nor delayed fluorescence. In solid state, the IC process was greatly suppressed, and the singlet excited state could undergo ISC process to achieve triplet excited state, which returned back to singlet excited state for delayed fluorescence, on the premise that the energy levels of singlet and triplet excited states were suitable. After wise molecular engineering, these processes could happen at higher energy electronic excited state rather than lowest energy excited state, namely the emission behaviors of AIDF molecules could disobeyed Kasha's rule. On the other hand, owing to the highly twisted conformations and weak intermolecular interactions of these AIDF materials, the short-range Dexter energy transfer that dominated the concentration-caused exciton annihilation could be diminished effectively. Thus, the efficiency roll-off of the nondoped OLEDs of AIDF materials was extremely small. This could be regarded as a breakthrough in addressing the serious efficiency roll-off of OLEDs based on common TADF emitters.

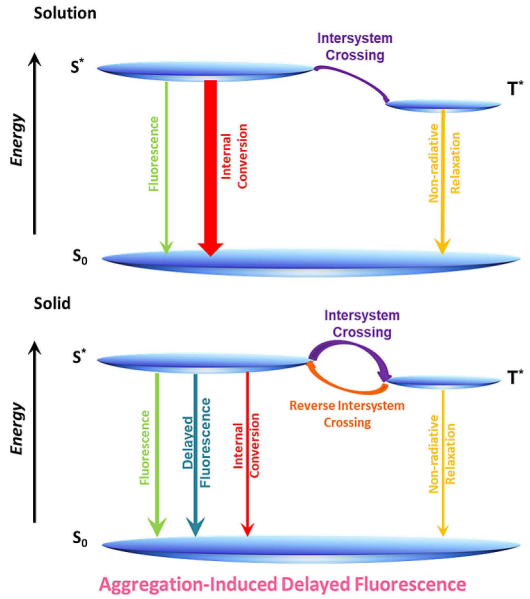

Figure 3. Photoluminescence process of AIDF materials in solution and in solid. Adapted with permission from Ref. [16], copyright 2018 Wiley-VCH.

3. Highly Efficient AIDF Materials and Nondoped OLEDs

The asymmetrical D-A-D′ structure gives high possibilities to combine different groups with specific functions. To further improve the carrier transport ability of the luminescent materials, 9-phenyl-9H-carbazole was selected to construct new AIDF materials, CP-BP-PXZ, CP-BP-PTZ and CP-BP-DMAC.[17] These AIDF materials had good thermal stability with high thermal decomposition temperatures (354–407 °C) and high glass-transition temperatures (99–105 °C). They showed PL peaks at 530, 538 and 490 nm, respectively, which were barely varied in comparison with those of DBT-BZ-PXZ, DBT-BZ-PTZ and DBT-BZ-DMAC, implying that the major fragments responsible for light emission probably were those consisting of BP and PXZ, PTZ, and DMAC. The PL intensities of CP-BP-PXZ, CP-BP-PTZ, and CP-BP-DMAC were greatly increased from THF solutions to neat films, and the PLQY of neat films reached 58.0, 45.3 and 67.4%, respectively. The ratios of prompt components (R_{prompt}) in THF solutions were very high (85–100%), but as the aggregate formation, the ratios of delayed components ($R_{delayed}$) increased, validating again that the delayed fluorescence was induced by aggregate formation. Encouraged by the prominent AIDF characteristics, nondoped OLEDs with a simple three-layer configuration of ITO/TAPC (25 nm)/emitter (35 nm)/TmPyPB (55 nm)/LiF (1 nm)/Al were fabricated by vacuum deposition. The turn-on voltages of these nondoped OLEDs were 2.5–2.7 V, suggesting efficient carrier injection and transport into the emitting layers (Figure 4). The further evaluation of bipolar potential by single-carrier devices also indicated the balanced carrier injection and recombination in these AIDF materials. The devices achieved excellent EQE_{max}, CE_{max} and PE_{max} of up to 18.4%, 59.1 cd A^{-1} and 65.7 lm W^{-1}, respectively, with small roll-off down to 0.2%.

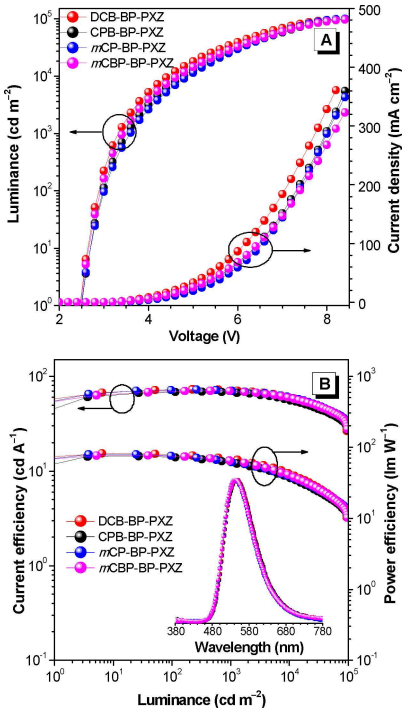

Figure 4. (A) Luminance-voltage-current density and (B) current efficiency-luminance-power efficiency curves of nondoped OLEDs. Inset in (B): EL spectra at luminance of 5000 cd m^{-2}. Adapted with permission from Ref. [18], copyright 2018 Wiley-VCH.

The effective design strategy of AIDF materials that ensured the realization of high-performance nondoped OLEDs was emerging as a research topic of increasing interest. By analyzing functions of host materials used in general doped OLEDs, we further designed a series of novel AIDF materials by introducing AIDF fragments, such as BP-PXZ, to common host materials, such as 1,4-di(carbazol-9-yl)benzene (DCB), 1,3-bis (carbazol-9-yl)benzene (*m*CP), 3,3′-di(carbazol-9-yl)biphenyl (*m*CBP) and CBP.[18] Thanks to the brilliant photophysical properties (PLQY: 66.0–71.6%; ΔE_{ST}: 0.016–0.024 eV), highly efficient nondoped OLEDs were attained based on these AIDF materials. The efficient carrier injection and transport into AIDF emitters were demonstrated by the low turn-on voltages of ~2.5 V as well as comparable hole and electron mobilities in single-carrier devices. They also showed excellent CE_{max} and PE_{max} of 69–72.9 cd A^{-1} and 75.0–81.8 lm W^{-1}, respectively. Meanwhile, the EQE_{max} reached 21.4–22.6%, with negligible decline at 1000 cd m^{-2} (19.2–20.1%), demonstrating nearly unity exciton utilization and remarkable efficiency stability. The combination of host materials and AIDF fragments could make advances in AIDF materials and paved a new avenue towards high-performance nondoped OLEDs.

General approach to fabricate highly efficient OLED devices is vacuum deposition which requires a relatively complicated process with high cost and precise engineering. In comparison, solution process developed in recent years such as spin-coating and inkjet printing are considered as low cost and high efficiency methods to be applied in OLEDs fabrication.[19] The recently developed solution-processible OLEDs were based on luminescent polymers, which had good film forming ability by solution-process technique.[20] But these polymers often encountered metal catalyst residue, structural defects inside polymers, and low reproducibility which undermined EL performance. In that case, some novel solution-processed small organic molecules with AIDF nature had been designed. We developed two solution-processed AIDF materials CC6-DBP-PXZ and CC6-DBP-DMAC by introducing a soft alkyl chain to the 9-position of carbazole. These materials could form smooth films by spin-coating technique. They possessed apparent AIDF characteristics with PLQY of 38.3 and 59.5% and very small ΔE_{ST} of 0.02 eV and 0.04 eV in spin-coated neat films, respectively. The nondoped OLEDs based on the spin-coated film of CC6-DBP-DMAC had an EQE_{max} of 9.02%. More importantly, the efficiency roll-off of this device was as small as 4.8% at 5000 cd m^{-2}, which was much superior to those of reported solution-processed OLEDs based on TADF emitters.[21] This work might provide an easy and efficient approach to solution-processed AIDF materials, which could have large potential in massive commercialization.

Recently, in addition to typical AIDF materials containing an electron-withdrawing BP core as discussed above, more and more AIDF materials with quite different molecular structures had been reported, such as derivatives from diphenylsulfone,[22] dibenzothiophene-S,S-dioxide,[10] quinoxaline,[23] xanthone,[24] phenothiazine-5,5-dioxide,[25] anthraquinone,[26] triazine,[27] and so forth (Figure 5).[28] These materials also showed advances in

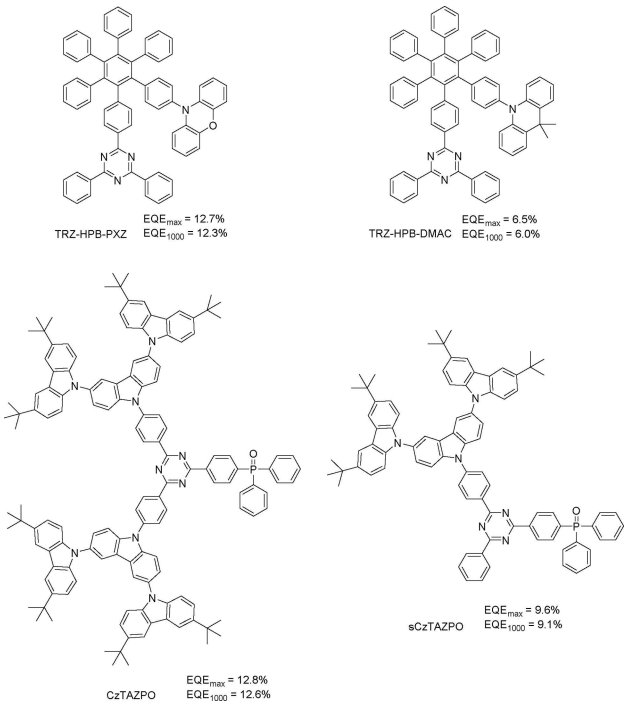

Figure 5. Molecular structures of solution-processed AIDF materials and key performance parameters: maximum EQE (EQE_{max}), and EQE at 1000 cd m^{-2} (EQE_{1000}).

constructing nondoped OLEDs with suppressed efficiency roll-off, which had been described in recent literatures.[29] Some new examples are presented below. We designed two new AIDF materials, TRZ-HPB-PXZ and TRZ-HPB-DMAC, by grafting electron donors (DMAC and PXZ) and acceptors (triazine) to an AIE-active hexaphenylbenzene (HPB) core that had efficient through-space conjugation character.[30] In these two materials, the HOMOs and LUMOs could be efficiently separated, but the spatially proximate molecular orbitals allowed through-space charge transfer, realizing very small ΔE_{ST} of 0.02 and 0.09 eV and high PLQY of 61.5 and 51.8%. The nondoped OLED of TRZ-HPB-PXZ with a configuration ITO/HATCN (5 nm)/TAPC (20 nm)/TCTA (5 nm)/TRZ-HPB-PXZ (35 nm) /TmPyPB (55 nm)/LiF (1 nm)/Al, in which dipyrazino[2,3-f:2′,3′-h]quinoxaline-2,3,6,7,10,11-hexacarbonitrile (HATCN), TAPC, 4,4′,4′′-tris(carbazol-9-yl)-triphenylamine (TCTA) and TmPyPB functioned as hole injection, hole-transporting, exciton-blocking and electron-transporting layers, respectively, reached an EQE_{max} of 12.3% with small efficiency roll-off 2.7% at 1000 cd m^{-2}, indicative of the good efficiency stability. Besides, Wang et al. designed two solution-processible AIDF materials CzTAZPO and sCZTAZPO with a dendritic structure.[31] The dendrites of the molecules displayed highly twisted conformation, providing positive condition for AIDF phenomenon. The OLEDs based on spin-coated films of two AIDF materials showed good EL performance with EQE_{max} values of 12.8% for CzTAZPO, and 9.1% for sCzTAZPO. Meanwhile, they exhibited small efficiency roll-off 1.8 and 0.97% at 1000 cd m^{-2}.

4. Conclusion

Nowadays, the efficient nondoped OLEDs can be an alternative technique for color display and white lighting in view of their increased efficiency stability, simplified device configurations and fabrication procedures, and reduced production cost. The development of luminescent materials for nondoped OLEDs remains as a challenge due to the concentration-caused quenching and exciton annihilation occurred in mainstream materials. Herein, a new class of purely organic AIDF materials with excellent performances in nondoped OLEDs are described. These intriguing AIDF materials are induced to emit prominent delayed fluorescence in the aggregated state, and demonstrate reduced ΔE_{ST}s and shortened lifetimes in neat films relative to doped films. They can harvest nearly 100% of excitons in nondoped devices and afford remarkable EL efficiencies and extremely small efficiency roll-off at high luminance. Recent works have also indicated the feasibility of fabricating solution-processed OLEDs with AIDF materials, which can also realize very small efficiency roll-off. These advances clearly reveal the high competitiveness of AIDF materials in the area of organic luminescent materials for OLEDs.

But from another perspective, the peak EL efficiencies of AIDF materials in nondoped OLEDs are still somewhat inferior to those of TADF emitters in doped devices, particularly at low luminance. The improvements of PLQY and light out-coupling efficiency in neat films of AIDF materials can well address this issue. Besides, the emission colors of most AIDF materials are still in green and yellow regions, and high-quality blue AIDF materials are very rare. This requires new donors and acceptors as well as a wise combination. The recently proposed through-space conjugated molecules and large coplanar moieties may be good choices in designing AIDF materials. Therefore, these two aspects may be the research directions of AIDF materials and devices. We believe that the rapid development of AIDF materials could bring advancement in academic studies and industry applications of OLEDs, and hope this concept can provide a clear outlook of these interesting luminescent materials and attract more researchers to make efforts to this promising field.

Acknowledgements

This work was financially supported by the National Natural Science Foundation of China (21788102), the Guangdong Natural Science Funds for Distinguished Young Scholar (2014A030306035), the Natural Science Foundation of Guangdong Province (2019B030301003) , the Science and Technology Program of Guangzhou (201804020027), and the Innovation and Technology Commission of Hong Kong (ITCCNERC14SC01).

Conflict of Interest

The authors declare no conflict of interest.

Keywords: aggregation-induced delayed fluorescence · efficiency roll-off · electroluminescence · organic light emitting diodes · thermally activated delayed fluorescence

[1] a) H. Uoyama, K. Goushi, K. Shizu, H. Nakamura, C. Adachi, *Nature* **2012**, *492*, 234–238; b) D. Zhang, L. Duan, Y. Li, D. Zhang, Y. Qiu, *J. Mater. Chem. C* **2014**, *2*, 8191–8197; c) M. Kim, S. K. Jeon, S.-H. Hwang, J. Y. Lee, *Adv. Mater.* **2015**, *27*, 2515–2520; d) X.-K. Liu, Z. Chen, C.-J. Zheng, C.-L. Liu, C.-S. Lee, F. Li, X.-M. Ou, X.-H. Zhang, *Adv. Mater.* **2015**, *27*, 2378–2383; e) Y. Seino, S. Inomata, H. Sasabe, Y.-J. Pu, J. Kido, *Adv. Mater.* **2016**, *28*, 2638–2643; f) T.-A. Lin, T. Chatterjee, W.-L. Tsai, W.-K. Lee, M.-J. Wu, M. Jiao, K.-C. Pan, C.-L. Yi, C.-L. Chung, K.-T. Wong, C.-C. Wu, *Adv. Mater.* **2016**, *28*, 6976–6983;

[2] a) Q. Zhang, D. Tsang, H. Kuwabara, Y. Hatae, B. Li, T. Takahashi, S. Y. Lee, T. Yasuda, C. Adachi, *Adv. Mater.* **2015**, *27*, 2096–2100; b) P. Rajamalli, N. Senthilkumar, P. Gandeepan, P.-Y. Huang, M.-J. Huang, C.-Z. Ren-Wu, C.-Y. Yang, M.-J. Chiu, L.-K. Chu, H.-W. Lin, C.-H. Cheng, *J. Am. Chem. Soc.* **2016**, *138*, 628–634; c) X. He, T. Shan, X. Tang, Y. Gao, J. Li, B. Yang, P. Lu, *J. Mater. Chem. C* **2016**, *4*, 10205–10208; d) J. Li, D. Ding, Y. Tao, Y. Wei, R. Chen, L. Xie, W. Huang, H. Xu, *Adv. Mater.* **2016**, *28*, 3122–3130.

[3] a) S. Hirata, Y. Sakai, K. Masui, H. Tanaka, S. Y. Lee, H. Nomura, N. Nakamura, M. Yasumatsu, H. Nakanotani, Q. Zhang, K. Shizu, H. Miyazaki, C. Adachi, *Nat. Mater.* **2015**, *14*, 330–336; b) H. Kaji, H. Suzuki, T. Fukushima, K. Shizu, K. Suzuki, S. Kubo, T. Komino, H. Oiwa, F. Suzuki, A. Wakamiya, Y. Murata, C. Adachi, *Nat. Commun.* **2015**, *6*, 8476; c) B. S. Kim, J. Y. Lee, *Adv. Funct. Mater.* **2014**, *24*, 3970–3977; d) K. Masui, H. Nakanotani, C. Adachi, *Org. Electron.* **2013**, *14*, 2721–2726.

[4] a) J. Lee, N. Aizawa, M. Numata, C. Adachi, T. Yasuda, *Adv. Mater.* **2017**, *29*, 1604856; b) I. S. Park, K. Matsuo, N. Aizawa, T. Yasuda, *Adv. Funct. Mater.* **2018**, *28*, 1802031.

[5] J. Mei, N. Leung, R. Kwok, J. W. Y. Lam, B. Z. Tang, *Chem. Rev.* **2015**, *115*, 11718–11940.
[6] a) Z. Zhao, J. W. Y. Lam, B. Z. Tang, *J. Mater. Chem.* **2012**, *22*, 23726–23740; b) B. Chen, Y. Jiang, L. Chen, H. Nie, B. He, P. Lu, H. H. Y. Sung, I. D. Williams, H. S. Kwok, Z. Zhao, B. Z. Tang, *Chem. Eur. J.* **2014**, *20*, 1931–1939; c) G. Lin, H. Peng, L. Chen, H. Nie, W. Luo, Y. Li, S. Chen, R. Hu, A. Qin, Z. Zhao, B. Z. Tang, *ACS Appl. Mater. Interfaces* **2016**, *8*, 16799–16808; d) J. Yang, J. Huang, Q. Li, Z. Li, *J. Mater. Chem. C* **2016**, *4*, 2663–2684; e)
[7] a) H. Zhao, Z. Wang, X. Cai, K. Liu, Z. He, X. Liu, Y. Cao, S.-J. Su, *Mater. Chem. Front.* **2017**, *1*, 2039–2046; b) I. H. Lee, W. Song, J. Y. Lee, *Org. Electron.* **2016**, *29*, 22–26; c) S. Wang, X. Yan, Z. Cheng, H. Zhang, Y. Liu, Y. Wang, *Angew. Chem. Int. Ed.* **2015**, *54*, 13068–13072; *Angew. Chem.* **2015**, *127*, 13260–13264.
[8] X.-L. Chen, J.-H. Jia, R. Yu, J.-Z. Liao, M.-S. Yang, C.-Z. Lu, *Angew. Chem. Int. Ed.* **2017**, *56*, 15006–15009; *Angew. Chem.* **2017**, *129*, 15202–15205.
[9] a) S. Xu, T. Liu, Y. Mu, Y.-F. Wang, Z. Chi, C.-C. Lo, S. Liu, Y. Zhang, A.L ien, J. Xu, *Angew. Chem. Int. Ed.* **2015**, *54*, 874–878; *Angew. Chem.* **2015**, *127*, 888–892; b) Z. Xie, C. Chen, S. Xu, J. Li, Y. Zhang, Si. Liu, J. Xu, Z. Chi, *Angew. Chem. Int. Ed.* **2015**, *54*, 7181–7184; *Angew. Chem.* **2015**, *127*, 7287–7290.
[10] S. Gan, W. Luo, B. He, L. Chen, H. Nie, R. Hu, A. Qin, Z. Zhao, B. Z. Tang, *J. Mater. Chem. C* **2016**, *4*, 3705–3708.
[11] R. Furue, T. Nishimoto, I. S. Park, J. Lee, T. Yasuda, *Angew. Chem. Int. Ed.* **2016**, *55*, 1–6; *Angew. Chem.* **2016**, *128*, 1–1.
[12] S. Y. Lee, T. Yasuda, Y. S. Yang, Q. Zhang, C. Adachi, *Angew. Chem. Int. Ed.* **2014**, *53*, 6520–6524.
[13] J. Guo, X.-L. Li, H. Nie, W. Luo, S. Gan, S. Hu, R. Hu, A. Qin, Z. Zhao S.-J. Su, B. Z. Tang, *Adv. Funct. Mater.* **2017**, *27*, 1606458.
[14] J. Guo, X.-L. Li, H. Nie, W. Luo, R. Hu, A. Qin, Z. Zhao, S.-J. Su, B. Z. Tang, *Chem. Mater.* **2017**, *29*, 3623–3631.
[15] J. Zeng, J. Guo, H. Liu, J. W. Y. Lam, Z. Zhao, S. Chen, B. Z. Tang, *Chem. Asian J.* **2019**, *14*, 8282–835.
[16] J. Guo, J. Fan, L. Lin, J. Zeng, H. Liu, C.-K. Wang, Z. Zhao, B. Z. Tang *Adv. Sci.* **2019**, *6*, 1801629.
[17] J. Huang, H. Nie, J. Zeng, Z. Zhuang, S. Gan, Y. Cai, J. Guo, S.-J. Su, Z. Zhao, B. Z. Tang, *Angew. Chem. Int. Ed.* **2017**, *56*, 12971–12976; *Angew. Chem.* **2017**, *129*, 13151–13156.
[18] H. Liu, J. Zeng, J. Guo, H. Nie, Z. Zhao, B. Z. Tang, *Angew. Chem. Int. Ed.* **2018**, *57*, 9290–9294; *Angew. Chem.* **2018**, *130*, 9434–9438.
[19] a) X. Liao, X. Yang, R. Zhang, J. Cheng, J. Li, S. Chen, J. Zhu, L. Li, *J. Mater. Chem. C* **2017**, *5*, 10001–10006; b) Y. Li, G. Xie, S. Gong, K. Wu, C. Yang, *Chem. Sci.* **2016**, *7*, 5441–5447; c) Y. Zou, S. Gong, G. Xie, C. Yang, *Adv. Opt. Mater.* **2018**, *6*, 1800568
[20] a) J. Luo, G. Xie, S. Gong, T. Chen, C. Yang, *Chem. Commun.* **2016**, *52*, 2292–2295; b) G. Xie, J. Luo, M. Huang, T. Chen, K. Wu, S. Gong, C. Yang, *Adv. Mater.* **2017**, *29*, 1604223. c) Y. Zhu, Y. Zhang, B. Yao, Y. Wang, Z. Zhang, H. Zhan, B. Zhang, Z. Xie, Y. Wang, Y. Cheng, *Macromolecules* **2016**, *49*, 4373–4377.
[21] J. Huang, Z. Xu, Z. Cai, J. Guo, J. Guo, P. Shen, Z. Wang, Z. Zhao, D. Ma, B. Z. Tang, *J. Mater. Chem. C* **2019**, *7*, 330–339.
[22] J. Zhao, X. Chen, Z. Yang, T. Liu, Z. Yang, Y. Zhang, J. Xu, Z. Chi, *J. Phys. Chem. C* **2019**, *123*, 1015–1020.
[23] a) L. Yu, Z. Wu, G. Xie, W. Zeng, D. Ma, C. Yang, *Chem. Sci.* **2018**, *9*, 1385–1391; b) L. Yu, Z. Wu, G. Xie, C. Zhong, Z. Zhu, D. Ma, C. Yang, *Chem. Commun.* **2018**, *54*, 1379–1382.
[24] a) J. Lee, N. Aizawa, M. Numata, C. Adachi, T. Yasuda, *Adv. Mater.* **2017**, *29*, 1604856; b) N. Aizawa, C.-J. Tsou, I. S. Park, T. Yasuda, *Polym. J.* **2017**, *49*, 197–202.
[25] S. Xiang, Z. Huang, S. Sun, X. Lv, L. Fan, S. Ye, H. Chen, R. Guo, L. Wang, *J. Mater. Chem. C* **2018**, *6*, 11436–11443.
[26] B. Huang, Y. Ji, Z. Li, N. Zhou, W. Jiang, Y. Feng, B. Lin, Y. Sun, *J. Lumin.* **2017**, *187*, 414–420.
[27] S. Y. Park, S. Choi, G. E. Park, H. J. Kim, C. Lee, J. S. Moon, S. W. Kim, S. Park, J. H. Kwon, M. J. Cho, D. H. Choi, *ACS Appl. Mater. Interfaces* **2018**, *10*, 14966–14977.
[28] a) Y. Chen, S. Wang, X. Wu, Y. Xu, H. Li, Y. Liu, H. Tong, L. Wang, *J. Mater. Chem. C* **2018**, *6*, 12503–12508; b) X. Chen, Z. Yang, Z. Xie, J. Zhao, Z. Yang, Y. Zhang, M. P. Aldred, Z. Chi, *Mater. Chem. Front.* **2018**, ***2***, 1017–1023; c) N. V. Nghia, S. Jana, S. Sujith, J. Y. Ryu, J. Lee, S. U. Lee, M. H. Lee, *Angew. Chem. Int. Ed.* **2018**, *57*, 12483–12488; d) X. Wang, S. Wang, J. Lv, S. Shao, L. Wang, X. Jing, F. Wang, *Chem. Sci.* **2019**, *10*, 2915–2923.
[29] J. Guo, Z. Zhao, B. Z. Tang, *Adv. Opt. Mater.* **2018**, *6*, 1800264.
[30] P. Zhang, J. Zeng, J. Guo, S. Zhen, B. Xiao, Z. Wang, Z. Zhao, B. Z. Tang, *Front. Chem.* **2019**, *7*, 199.
[31] J. Wang, C. Liu, C. Jiang, C. Yao, M. Gu, W. Wang, *Org. Electron.* **2019**, *65*, 170–178.

Manuscript received: April 16, 2019
Revised manuscript received: May 12, 2019
Accepted manuscript online: May 16, 2019
Version of record online: June 27, 2019